J Appl Physiol
91: 986–994, 2001.

highlighted topics

Signal Transduction in Smooth Muscle
Selected Contribution: Time course and heterogeneity of contractile responses in cultured human airway smooth muscle cells

BEN FABRY,[1] GEOFFREY N. MAKSYM,[2] STEPHANIE A. SHORE,[1] PAUL E. MOORE,[1] REYNOLD A. PANETTIERI, JR. ,[3] JAMES P. BUTLER,[1] AND JEFFREY J. FREDBERG[1]
[1]*Physiology Program, Harvard School of Public Health, Boston, Massachusetts 02115;* [2]*School of Biomedical Engineering, Dalhousie University, Halifax, Nova Scotia, Canada B3H 3J5; and* [3]*Pulmonary and Critical Care Division, University of Pennsylvania School of Medicine, Philadelphia, Pennsylvania 19104*

Received 9 February 2001; accepted in final form 19 April 2001

Fabry, Ben, Geoffrey N. Maksym, Stephanie A. Shore, Paul E. Moore, Reynold A. Panettieri, Jr., James P. Butler, and Jeffrey J. Fredberg. Selected Contribution: Time course and heterogeneity of contractile responses in cultured human airway smooth muscle cells. *J Appl Physiol* 91: 986–994, 2001.—We measured the time course and heterogeneity of responses to contractile and relaxing agonists in individual human airway smooth muscle (HASM) cells in culture. To this end, we developed a microrheometer based on magnetic twisting cytometry adapted with a novel optical detection system. Ferromagnetic beads (4.5 μm) coated with Arg-Gly-Asp peptide were bound to integrins on the cell surface. The beads were twisted in a sinusoidally varying magnetic field at 0.75 Hz. Oscillatory bead displacements were recorded using a phase-synchronized video camera. The storage modulus (cell stiffness; G′), loss modulus (friction; G″), and hysteresivity (η; ratio of G″ to G′) could be determined with a time resolution of 1.3 s. Within 5 s after addition of histamine (100 μM), G′ increased by 2.2-fold, G″ increased by 3.0-fold, and η increased transiently from 0.27 to 0.34. By 20 s, η decreased to 0.25, whereas G′ and G″ remained above baseline. Comparable results were obtained with bradykinin (1 μM). These changes in G′, G″, and η measured in cells were similar to but smaller than those reported for intact muscle strips. When we ablated baseline tone by adding the relaxing agonist dibutyryl cAMP (1 mM), G′ decreased within 5 min by 3.3-fold. With relaxing and contracting agonists, G′ could be manipulated through a contractile range of 7.3-fold. Cell populations exhibited a log-normal distribution of baseline stiffness (geometric SD = 2.8) and a heterogeneous response to both contractile and relaxing agonists, partly attributable to variability of baseline tone between cells. The total contractile range of the cells (from maximally relaxed to maximally stimulated), however, was independent of baseline stiffness. We conclude that HASM cells in culture exhibit a clear, although heterogeneous, response to contractile and relaxing agonists and express the essential mechanical features characteristic of the contractile response observed at the tissue level.

cell mechanics; muscle contraction; muscle relaxation; actin; myosin; bridge dynamics; cytoskeleton

SMOOTH MUSCLE (SM) cells in culture serve as an essential tool for studying the pathophysiology of widespread human diseases such as bronchial asthma and hypertension. Compared with SM cells studied at the tissue level, SM cells in culture offer a number of practical advantages. For example, culture systems are not influenced by the presence of other cell types, they can be more easily transfected, they can be probed at different stages during their cell cycle, and the extracellular milieu and the cell substrate are in the hands of the experimenter. Nonetheless, contraction, the key mechanical end point of SM function, has been difficult to characterize in cell culture systems because adhesion of the cells to the dish makes measurements of force development and shortening problematic.

One approach that has been applied successfully to measure mechanical responses in cultured human airway smooth muscle (HASM) cells is magnetic twisting cytometry (MTC) (12, 15, 16, 19). For example, Hubmayr et al. (12) reported that agonists that increase intracellular Ca^{2+} concentration or inositol trisphosphate formation in cultured HASM cells cause a dose-

Address for reprint requests and other correspondence: B. Fabry, Physiology Program, Harvard School of Public Health, 665 Huntington Ave., Boston, MA 02115 (E-mail:bfabry@hsph.harvard.edu).

The costs of publication of this article were defrayed in part by the payment of page charges. The article must therefore be hereby marked "*advertisement*" in accordance with 18 U.S.C. Section 1734 solely to indicate this fact.

dependent increase in cell stiffness, and agonists that increase intracellular cAMP and cGMP formation in those cells cause a dose-dependent decrease in cell stiffness. MTC probes these changes in cell mechanical properties using magnetic microbeads (4.5 μm diameter), which are coated with ligands for specific cell surface receptors; if the beads are coated with an Arg-Gly-Asp (RGD)-containing peptide, they will firmly connect via integrin receptors to the cytoskeleton (28). The RGD-coated beads are first magnetized in the horizontal direction by application of a brief and strong magnetic pulse. A homogeneous magnetic "twisting" field is then applied in the vertical direction, which creates a torque on the beads. This magnetic torque causes the beads to rotate (like a compass needle in the earth's magnetic field) and thus to deform the cytoskeleton. As the cytoskeleton deforms, mechanical stresses are generated within it, which tend to oppose bead rotation. The higher the cell's elastic modulus, the larger the mechanical stress developed for a given degree of bead rotation. Thus a large rotation indicates a small elastic modulus of the cell and vice versa. When the beads are twisted in a sinusoidally varying magnetic field, the cells' mechanical properties can be characterized in terms of a storage modulus (stiffness; G′) and a loss modulus (friction; G″) as defined below (16). Sinusoidal twisting can also be used to track changes of cell mechanical properties over time as G′ and G″ are computed for each twisting cycle.

It has been demonstrated at the level of intact muscle tissue strips that G′ and the ratio of G″ to G′ [hysteresivity (η)] undergo characteristic changes during a contractile event, particularly a rapid increase in G′ and a transient increase in η (7). The rapid increase in G′ has been interpreted as reflecting increased numbers of actomyosin bridges, and the transient in η has been interpreted as reflecting changes in bridge detachment rate (7). At the level of cultured cells, such changes in G′ have also been reported (15, 16, 19, 24), but changes in η, if they exist, have not been resolved with existing techniques (16).

Our aim in this report was to assess the extent to which SM cells in culture recapitulate those essential mechanical features of SM contraction and, in addition, the extent to which individual cells exhibit a heterogeneous mechanical behavior. For that purpose, we measured the response of individual cultured HASM cells using MTC with sinusoidal twisting, combined with a novel optical method to quantify bead motion. We found that HASM cells in culture exhibit responses that are markedly heterogeneous; however, they express both the rapid increase in stiffness and the transient increase in η. We conclude that HASM cells in culture express the essential mechanical features that are characteristic of the contractile response observed at the level of intact muscle tissue.

METHODS

Cell culture. Human tracheas were obtained from lung transplant donors, in accordance with procedures approved by the University of Pennsylvania Committee on Studies Involving Human Beings. Tracheal SM cells were harvested as previously described (20). The cells were cultured on plastic in Ham's F-12 medium supplemented with 10% fetal bovine serum, 100 U/ml of penicillin, 100 μg/ml of streptomycin, 200 μg/ml of amphotericin B, 12 mM NaOH, 1.7 μM $CaCl_2$, 2 mM L-glutamine, and 25 mM HEPES. The medium was replaced every 3–4 days, and cells were passaged every 10–14 days (15). Confluent cells were serum deprived and supplemented with 5.7 μg/ml insulin and 5 μg/ml transferrin 24 h before the experiments. We used cells in *passages 5–7* from four different donors. The experiments described here were carried out on 7 experimental days, with cells from each donor being measured in two to six cell wells for each treatment.

Cell-bead preparation. Cells were harvested by a brief exposure to 0.25% trypsin and 1 mM EDTA and plated in 6.4-mm plastic wells (Removawell strips, Dynex, Chantilly, VA) at a density of ~20,000 cells/well. Measurements of cellular mechanics were performed 3–6 h later. The plastic wells were coated with collagen I (500 ng/cm^2) at least 24 h before plating.

Ferromagnetic beads (diameter of 4.5 μm, produced as described in Ref. 18) were coated with a synthetic RGD (Arg-Gly-Asp)-containing peptide (Peptite 2000, Integra Life Sciences, San Diego, CA). Coating density was 50 μg peptide per milligram of beads in 1 ml of carbonate buffer (pH 9.4). The beads were suspended in serum-free medium, and ~20,000 beads were added to an individual cell well. After a 15- to 20-min incubation at 37°C to allow for binding of the beads to integrins on the cell surface, the well was washed twice with serum-free medium to remove unbound beads. The cell well was then placed on the microscope stage for determination of mechanical properties.

Torque application. A pair of magnetizing coils and twisting coils were mounted to a microscope stage (Fig. 1*A*). The microscope stage was heated to maintain a constant temperature of 37°C. The twisting current was provided by a current source that was driven by a microcontroller. The magnetizing current was generated by discharging a 16-μF capacitor (charged to 1,500 V) through the magnetizing coils. The magnetizing coils were connected in parallel with a high-voltage, fast-recovery diode to prevent current oscillations between the capacitor and the coil. Under microscopic observation, the beads were magnetized horizontally and twisted in a vertically aligned homogenous magnetic field.

During twisting, the magnitude of the specific torque (T) (mechanical torque per unit bead volume[1]) applied to a bead by the magnetic field (H) is

$$T = cH \cos \alpha \quad (1)$$

where $\pi/2 - \alpha$ is the angle of the bead's magnetic moment relative to the twisting field (this choice of α means that, for an initial angle of $\alpha = 0$, the final angle α also represents the angular rotation). The c is the bead constant, expressed as torque per unit bead volume per gauss; c is determined by placing beads in a fluid of known viscosity and measuring the angular velocity while twisting (27). Throughout this study, we used beads with $c = 1.86$ Pa/G. Unless noted otherwise, we applied a sinusoidal twisting field of 20 G at a frequency of 0.75 Hz, which resulted in a specific torque amplitude of 37.2 Pa.

[1]Note that, in previous publications, T has sometimes been defined as the mechanical torque per unit bead volume, divided by a shape factor (6 for spherical beads).

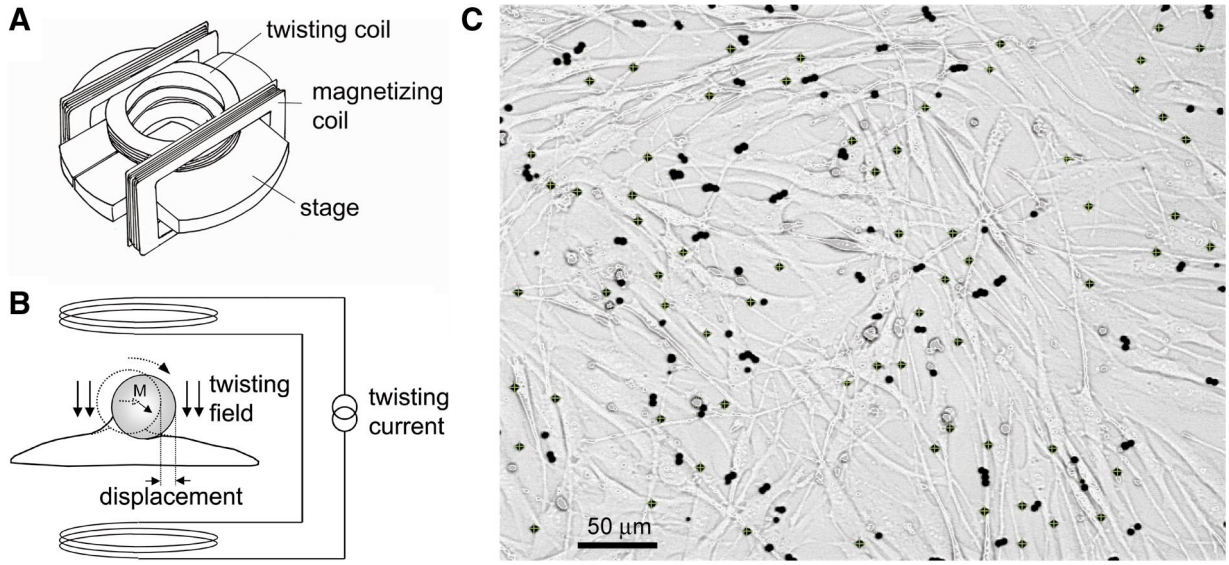

Fig. 1. *A*: microscope stage with twisting coils and magnetization coils. *B*: a homogeneous magnetic twisting field causes the bead to rotate and to displace. M denotes the direction of the bead's magnetic moment. *C*: image of cultured human airway smooth muscle (HASM) cells with magnetic beads. Beads marked with a green cross have been automatically recognized by an image-processing algorithm.

The magnetic twisting field causes both a rotation and a pivoting displacement of the beads (Fig. 1*B*). For small bead motion, rotation and displacement are linearly related, as verified using a finite element analysis (S. Mijailovich, personal communication). The relationship between rotation and displacement is modulated by the degree of bead internalization (6).

Image acquisition. We used an inverted microscope (Nikon Diaphot) with a ×10 objective (numerical aperture of 0.2). The microscope was placed on a vibration isolation table (Newport, Irvine, CA). A progressive scan, triggerable black and white charge-coupled device camera with pixel-clock synchronization (JAI CV-M10, Glostrup, Denmark) was attached to the camera sideport of the microscope via a camera adapter with ×1 magnification. The resulting field of view was 450 μm × 350 μm (Fig. 1*C*). Image acquisition was phase locked to the sinusoidal twisting field so that 16 images were obtained during a twisting cycle. Images were amplified, digitized, and transferred to the PC memory using a frame grabber (PC Eye 4, Eltec, Mainz, Germany).

Image analysis. After the first image of a sequence was acquired and transferred into the computer memory, a simple pattern recognition algorithm searched for single isolated beads that fell within a specified range of size, contrast, and shape. Beads appear black on a white background. Because the intensity of a pixel can have a value between 0 (black) and 255 (white), we specified that *1*) the center of a bead must have an intensity of <80, *2*) all pixels within a radius of 1.75 μm from the bead center must have an intensity of <170, and *3*) all pixels outside a radius of 2.75 μm from the bead center and within a radius of 7 μm must have an intensity of >170. This ensured that the minimum qualifying distance between two beads was more than two bead diameters, or 9 μm. The black and white level of the video signal was manually adjusted so that the image of the beads (but not the image of the surrounding cells) utilized as much of the 8-bit resolution of the frame grabber as possible. After identification of the beads, a bead-tracking algorithm computed the intensity-weighted center of mass of the bead within a rectangular window (12 × 12 pixels) using the equation

$$\bar{x} = \frac{\sum_{k}^{\text{window}} x_k(170 - \mathrm{I}_k)}{\sum_{k}^{\text{window}} (170 - \mathrm{I}_k)} \quad \text{for } \mathrm{I}_k \leq 170 \qquad (2)$$

where $\bar{x}$ is the x-coordinate of the bead's center, I_k is the intensity, and x_k is the x-coordinate of the kth pixel within the window. The same algorithm with the y-coordinates of the pixels was then applied to compute the y-coordinate of the bead's center ($\bar{y}$). Pixels with an intensity above 170 were considered as background and were ignored. With the use of this algorithm, the bead position could be determined with an accuracy of 5 nm (root mean square). If a bead moved partially outside the window, the window was repositioned around the newly computed (but erroneous) bead center, and the center-of-mass algorithm was repeated until the difference in bead position between two subsequent iterations was <0.1 nm. The bead-tracking algorithm excluded beads from further analysis if they moved by more than 3.5 μm (i.e., if more than one-half of the bead moved outside the window). For each subsequent image, the bead-tracking algorithm repositioned the window around the bead's center as computed from the previous image. Bead tracking could be executed on-line, since the analysis of one image required only 15 ms of computation time on a PC (450 MHz Pentium II) for an image containing ~100 beads. Consequently, only bead positions were recorded, but images were not.

Determining cell rheological parameters. We used Fourier transformation of the bead motion signal ($\tilde{x}$) and the specific torque ($\tilde{\mathrm{T}}$) to compute a complex modulus (G), defined here as

$$\mathrm{G} = \tilde{\mathrm{T}}/\tilde{x} = \mathrm{G}' + j\mathrm{G}'' = \mathrm{G}'(1 + j\eta) \qquad (3)$$

where G has dimensions of pascals per nanometer and is related by a geometric factor to the complex shear modulus of the cell, and j is the unit imaginary number $\sqrt{-1}$. The

component of bead displacement that is in phase with the magnetic torque corresponds to the real part of the complex modulus and is denoted G′. G′ is a measure of the elasticity or stiffness. The component of bead displacement that is out of phase with the magnetic torque corresponds to the imaginary part of the complex modulus and is denoted G″. G″ is a measure of the friction. We have also computed the η, which is the ratio of G″ to G′. We confirmed linear mechanical behavior of HASM cells by measuring the complex modulus at different torque amplitudes. We found that G′ and G″ did not change when specific torque amplitudes varied between 1.8 and 130.2 Pa and bead displacement amplitudes varied between 0.5 and 1,000 nm.

Protocol. Immediately after bead magnetization, the beads were twisted in a sinusoidal magnetic field of 20 G amplitude at 0.75 Hz. After 60 s, we instilled contractile or relaxing agonists [histamine, bradykinin, or dibutyryl cAMP (DBcAMP), diluted in 20 μl of warm medium] into the cell well (containing 100 μl of medium) using a micropipette. The final concentrations after mixing were 100 μM for histamine, 1 μM for bradykinin, and 1 mM for DBcAMP. We verified that this procedure guaranteed almost instantaneous mixing by instilling 20 μl of blue dye into a cell well containing 100 μl of water.

Reagents. Tissue culture reagents and drugs used in this study were obtained from Sigma Chemical (St. Louis, MO), with the exception of trypsin-EDTA solution, which was purchased from GIBCO (Grand Island, NY). Histamine, bradykinin, and DBcAMP were dissolved in distilled water at 10^{-1} M. All reagents were frozen in aliquots, thawed on the day of use, and diluted in media.

RESULTS

The storage modulus (G′) and loss modulus (G″) of HASM cells under baseline conditions remained stable when continuously monitored over 5 min. Median values from all data (n = 1,146 cells) show that, within 5 s after addition of the contractile agonist histamine (100 μM), G′ increased by 2.2-fold and G″ increased by 3.0-fold (Fig. 2); η transiently increased from 0.27 to 0.34 within 5 s and subsequently decreased to 0.25 within 20 s. After their rapid increase, both G′ and G″ slowly declined and, after 2 min, reached plateau values of 1.3-fold of baseline. All subsequent results for cell contraction (see Figs. 4–8) relate to early responses, defined here as the median of G′ or bead displacement amplitude measured between 5 and 15 s after histamine was given. We obtained responses similar to histamine when cells (originating from one donor, n = 177) were stimulated with bradykinin (1 μM). G′ increased by 3.9-fold, and G″ increased by 5.2-fold within 7 s; η transiently increased from 0.27 to 0.37 within 4 s and subsequently decreased to 0.24 within 20 s.

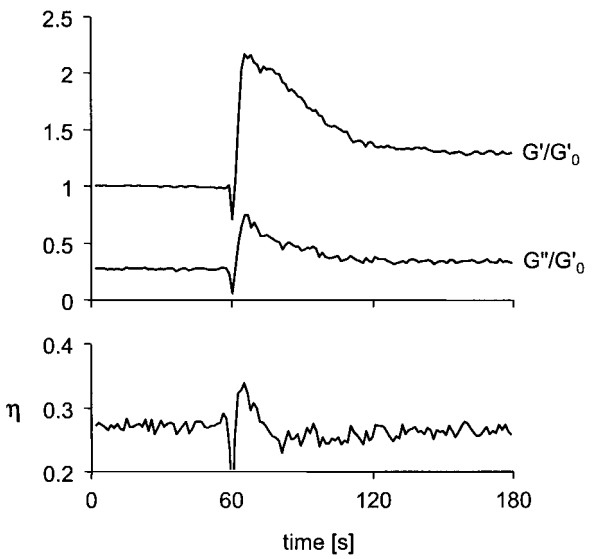

Fig. 2. Contractile response [median of cell stiffness (G′), friction (G″) and hysteresivity (η); n = 1,146] of HASM cells to histamine (100 μM) added at 60 s. For each cell, G′ and G″ were normalized to baseline G′0, defined as the median value of G′ measured over the first 55 s. The brief drop in all traces at 60 s is an artifact due to blocking of the microscope light path by the tip of a micropipette that was used to add histamine to the cell well.

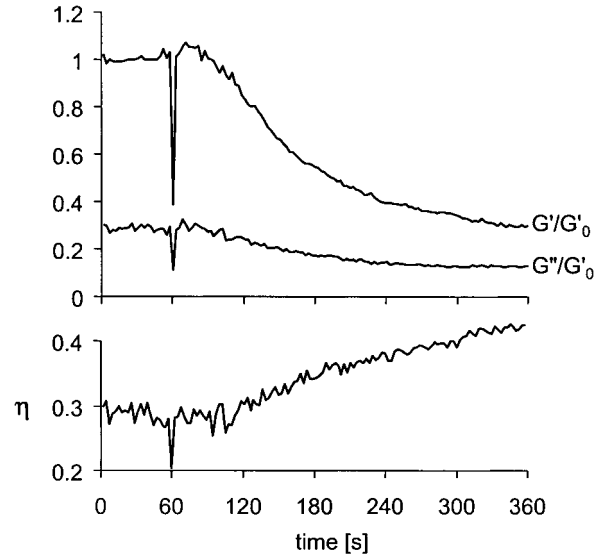

Fig. 3. Response to the relaxing agonist dibutyryl cAMP (DBcAMP; 1 mM) (median of G′, G″, and η; n = 554) added at 60 s. For each cell, G′ and G″ were normalized to baseline G′0.

Within 5 min after addition of the relaxing agonist DBcAMP (1 mM), a cell-permeable analog of cAMP, G′ decreased to 30%, G″ decreased to 45% of baseline values, and η increased from 0.28 to 0.42 (Fig. 3). This effect of DBcAMP suggests the existence of an appreciable level of baseline tone in these cells. All subsequent data on cell relaxation (see Figs. 4–8) relate to steady-state responses, defined here as the median of G′ or bead displacement amplitude measured between 4.5 and 5 min after DBcAMP was given.

Under baseline conditions, the amplitude of bead displacements (which is inversely proportional to the magnitude of G; |G|) varied widely between cells in each well. A histogram of all data revealed a distribution of bead displacement amplitudes that approximates a log-normal distribution (Fig. 4). Median displacement amplitude under baseline conditions was 57 nm (n = 1,700 beads), and the geometric standard deviation was 2.8. Within individual wells, the geometric standard deviation of bead displacement amplitude under baseline conditions was 2.5, indicating that well-

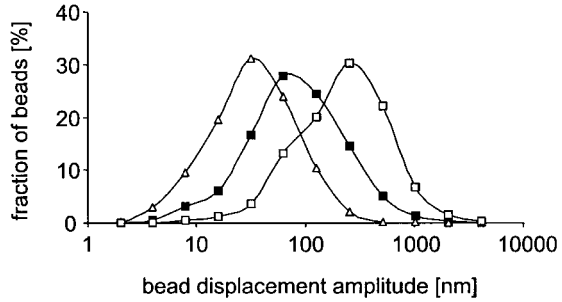

Fig. 4. Probability function of bead displacement amplitudes under baseline condition (■, n = 1,700), histamine (△, n = 1,146), and DBcAMP (□, n = 554). Bin widths (in nm) increased geometrically as 1, 2, 4, 8, and so forth.

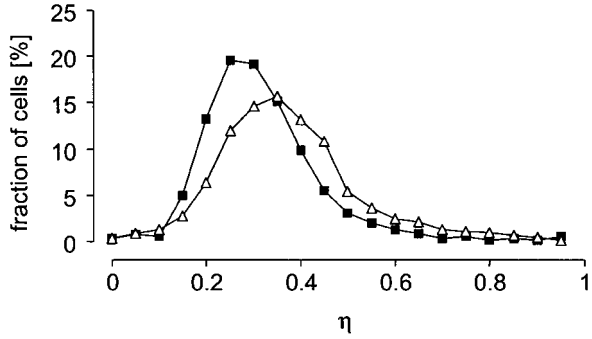

Fig. 6. Probability function of η at baseline (■) and in response to histamine (△, 100 μM); n = 1,146. Bin width Δη was 0.05. Baseline η for each cell was computed as the median η from 10 to 5 s before addition of histamine; η in response to histamine was computed as the median η from 3 to 8 s after addition of histamine.

to-well, day-to-day, and donor-to-donor variability contributed little to the total variability of bead displacement amplitude. When cells were treated with histamine (n = 1,146 beads), median bead displacement decreased to 24 nm, and geometric standard deviation decreased to 2.5. When cells were treated with DBcAMP (n = 554 beads), median bead displacement amplitude increased to 161 nm, whereas geometric standard deviation decreased to 2.6.

The changes in increase in stiffness (G′) relative to baseline observed in response to histamine and the changes in decrease of stiffness relative to baseline observed in response to DBcAMP also varied widely between cells (Fig. 5). A similarly wide distribution was found for values of G″ and |G| (data not shown). Generally, cells that exhibited a large increase in G′ also exhibited a large increase in G″. Thus cell-to-cell variability of η in response to histamine increased only slightly (Fig. 6). Over 90% of all cells that were treated with histamine increased stiffness by more than 25%, which we set here as a threshold to distinguish responding from nonresponding cells. Eighty-four percent of responding cells responded rapidly, with a stiffness increase that peaked during the first 10 s; 65% of responding cells exhibited a transient overshoot, i.e., a peak stiffness increase that was more than double the plateau stiffness increase (plateau stiffness was measured from 90 to 120 s after the onset of contraction).

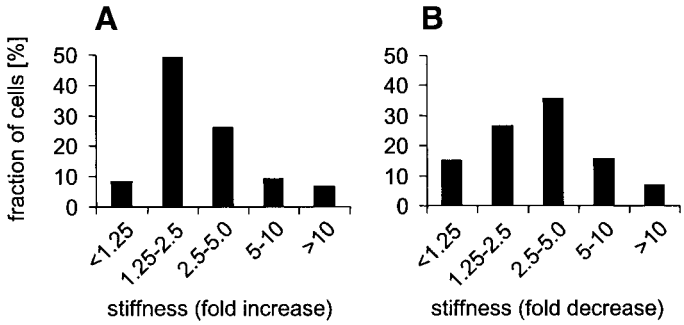

Fig. 5. Histogram of stiffness (fold change from baseline) in response to 100 μM histamine (*A*; n = 1,146) and 1 mM DBcAMP (*B*; n = 554). A 1.25-fold decrease corresponds to a value of 80% of baseline, a 2.5-fold decrease to 40% of baseline, and so forth.

When we plotted the displacement amplitude after challenge with histamine or DBcAMP for each bead vs. the baseline displacement amplitude, an interesting relationship became apparent (Fig. 7). Each datum in Fig. 7 represents one bead. Symbols above the line of identity indicate softening of the cell; symbols below the line of identity indicate stiffening of the cell. The exponent of the power-law regression for both drugs was significantly smaller than 1 ($P < 0.05$). This means that cells with lower baseline stiffness (i.e., with larger bead displacement amplitudes) tended to stiffen more, and those with higher baseline stiffness tended to stiffen less. With DBcAMP, the reverse was true: the cells with higher baseline stiffness softened more, and those with lower baseline stiffness softened less.

To further quantify the relationship between baseline stiffness and responses to contractile and relaxing agonists, we ranked the bead displacement amplitude before challenge and arranged the data into six groups so that the median of the bead displacement amplitude at baseline of each group was 10, 20, 40, 80, 160, and

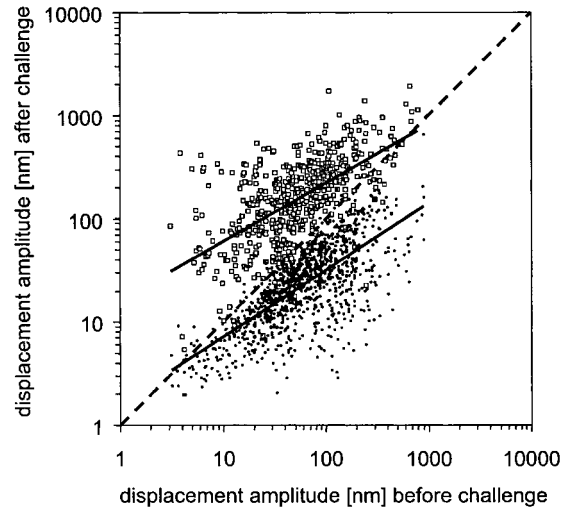

Fig. 7. Bead displacement amplitude after challenge with histamine (●, 100 μM, n = 1,146) and DBcAMP (□, 1 mM, n = 554) vs. baseline amplitude of bead displacement. Each symbol represents the data from one bead.

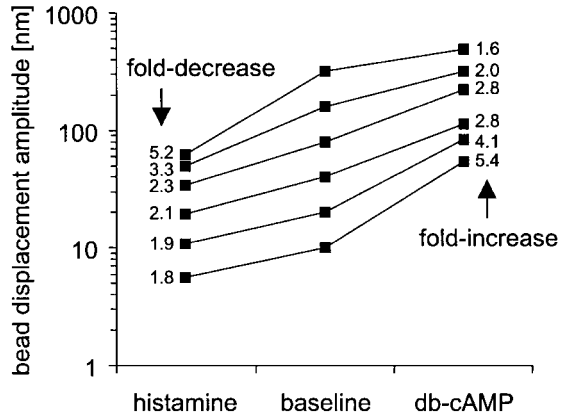

Fig. 8. Geometric mean of the bead displacement amplitude taken from corresponding cell groups before and after challenge with histamine and DBcAMP. The numbers next to the lines indicate the increase and decrease (in fold) in bead displacement amplitude due to challenge.

320 nm, respectively. For each group, we also computed the median of the bead displacement amplitude after challenge (Fig. 8). The slope of the line that connects the corresponding group entries is proportional to the change in the bead displacement amplitude relative to baseline (note the logarithmic ordinate). We found that cells in the stiffest group (i.e., with the smallest bead displacement amplitude at baseline) stiffened by only 1.8-fold in response to histamine, whereas cells in the softest group stiffened by 5.2-fold. Conversely, cells in the stiffest group decreased their stiffness by 5.4-fold in response to DBcAMP, whereas cells in the softest group decreased their stiffness by only 1.6-fold.

DISCUSSION

Our results demonstrated that HASM cells in culture rapidly increased stiffness and transiently increased η when challenged with contractile agonists. The cells also decreased their stiffness when treated with the relaxing agent DBcAMP. Both the baseline mechanical properties and responses to contractile and relaxing agonists varied widely between cells. In the following discussion, we briefly summarize other techniques that have been used to measure contractile responses in cultured cells and consider mechanisms that could be responsible for the time course and heterogeneity of those responses in cultured SM.

Mounting cells to a force transducer and a length driver is considered the most direct but technically the most complicated approach to measure force generation and thus contractility in individual SM cells (25, 30). This technique, however, cannot be applied to cells that remain adherent to a cell culture dish. Instead, a more indirect approach to characterize contractility is needed. In intact SM tissue, stiffness is closely related to force generation and is thought to reflect the number of attached actomyosin bridges (7, 31). The extent to which stiffness can be taken as a substitute for force generation in adherent SM cells in culture remains an open question; nonetheless, changes of stiffness in cultured HASM measured with MTC have been used to assess responses to contractile and relaxing agonists (12, 15, 16, 19, 24). The results reported in those studies support the notion of a direct effect of actomyosin bridges on cell stiffness: agents that are known to cause muscle contraction (e.g., histamine, acetylcholine, substance P, KCl) consistently cause a dose-dependent increase in cell stiffness, and agents that are known to cause relaxation (e.g., isoproterenol, forskolin, DBcAMP, prostaglandin E_2) consistently cause a dose-dependent decrease in cell stiffness (12).

MTC, as used most frequently in the past, derives cell stiffness from measurements of the rotation of ferromagnetic microbeads that are bound to specific receptors on the cell surface and twisted in a constant magnetic field (28); changes of the remanent magnetic field are used to compute an average rotation of several thousand beads that are attached to an approximately equal number of cells (27). MTC has also been combined with a sinusoidally varying twisting field, thus allowing for continuous measurements of cell stiffness (16). In a recent study, Maksym et al. (16) used a twisting frequency of 0.1 Hz to measure changes of cell mechanical parameters with a corresponding time resolution of 10 s. This time resolution, however, was not sufficient to reveal transients in η when HASM cells were stimulated with histamine. Data obtained with sinusoidal twisting also suggested that the mechanical properties of HASM cells might be very heterogeneous (16), but the nature of the technique did not allow this to be confirmed by direct observation.

In this study, we replaced magnetic sensing of average bead rotation in a cell population by a novel optical detection technique that allowed us to resolve the mechanical properties of individual cells and thus to quantify cell-to-cell heterogeneity of mechanical responses. MTC with optical detection of bead motion typically measured 50 cells simultaneously in one optical field and could identify and exclude loose beads or bead clusters from data analysis (Fig. 1*C*). This is important because loose beads and bead clusters can contribute to measurement artifacts in MTC with magnetic detection (6, 16). In addition to the ability to measure the responses of individual cells, MTC with optical detection achieved a time resolution of 1.3 s. This temporal resolution allowed us to detect transients in η that were not apparent in the prior study of Maksym et al. (16). The time course of mechanical responses to contractile and relaxing agonists and the heterogeneity of responses among cells are discussed separately below.

Time course of mechanical responses. When challenged with the contractile agonist histamine, we found that, within 5–8 s, HASM cells in culture increased their stiffness (G') by 2.2-fold and friction (G'') by 3.0-fold. The η increased from 0.27 to 0.34 within 5 s and then fell to 0.25 within 20 s. When cells were challenged with the relaxing agonist DBcAMP, we found that within 5 min G' decreased by 3.3-fold, G'' decreased by 2.2-fold, and η increased from 0.28 to

0.42. With two exceptions, these data are qualitatively consistent with those obtained in an earlier study by Maksym et al. (16) that used MTC with sinusoidal twisting and magnetic detection. First, in that study, no transient response of η was apparent when cells were challenged with histamine. On the basis of the results reported here, it is now clear that the MTC system used by Maksym et al. had insufficient temporal resolution to detect the η transient. Second, the study by Maksym et al. found no response in η when cells were exposed to DBcAMP. We speculate that this was due to an artifact caused by loosely coupled beads (6, 16). As cells become less stiff when challenged with DBcAMP, the fraction of beads that contribute to that artifact can increase. MTC with optical detection of bead motion excludes loosely coupled beads and thereby overcomes these limitations.

The time course of mechanical responses that we have measured in cultured HASM closely resembles that of SM observed at the tissue level; when activated by electric field stimulation, G′ and G″ rise sharply within the first 10 s; the η transiently increases within 4 s and then decays with a time constant of ~20 s (7). Although they are similar, the increases in G′, G″, and η in cultured HASM cells during activation are smaller than those observed in SM at the tissue level. A number of possibilities could account for this apparently reduced responsiveness of cultured cells. First, cultured SM cells exist in a partially dedifferentiated state and express a smaller ratio of contractile to noncontractile components of the cytoskeleton than do freshly isolated SM cells (9); therefore, cultured SM cells are likely to have a larger parallel elastic component and a diminished change in total stiffness during SM contraction (14). Second, HASM cells in culture, when observed between 3 and 6 h after plating, were not spindle shaped or aligned in parallel, as they are at the tissue level (5); instead, they were irregularly shaped (Fig. 1*C*). Thus we expect that the connection between the bead and the cell's contractile apparatus might be substantially less direct and, especially, less well aligned compared with SM tissue that has been longitudinally mounted and stretched between a force transducer and a length driver. Third, unstimulated (resting) HASM cells in culture exist in a partially contracted state (12, 24); we found that cells decreased stiffness typically by 3.3-fold in response to the relaxing agonist DBcAMP (Fig. 3). With the use of relaxing and contracting agonists, stiffness in HASM cells in culture could be manipulated through a total contractile range of 7.3-fold and in some cells considerably more (Fig. 5), which roughly compares with the range of 10- to 20-fold that is usually seen in airway SM tissue.

On the basis of the similarities between SM in culture vs. tissue in their time courses of G′, G″, and η during contraction, we speculate that underlying molecular processes and associated rate constants that govern contractile events might be similar. At the tissue level, changes in G′, G″, and η in response to contractile activation have been interpreted in the following way (7). The storage modulus G′ is related to the number of actomyosin bridges that are attached; this is because attached bridges store mechanical strain energy when stretched. The loss modulus G″ is related to the number of cross bridges that detach during the course of a stretch cycle; this is because the mechanical strain energy that was stored in attached bridges is lost to heat when they detach. For small strains, at least one molecule of ATP must be hydrolyzed for each cross-bridge detachment event (23). Therefore, G″ and the rate of ATP utilization are closely linked (2, 7, 13). The η is related to the rate of cross-bridge detachment (7). Because the rate of bridge detachment determines the maximum velocity (V_{max}) with which an activated muscle can shorten (13), it follows that V_{max} and η are also closely linked (2, 7). Thus key molecular processes during SM activation are mirrored by characteristic changes in mechanical properties observed at the tissue level; as the number of bridges during a contractile event increases, force and stiffness (G′) tend to increase in parallel. The number of detaching bridges and thus total ATP utilization also increase, which is reflected by an increasing G″. As rapidly cycling actomyosin cross bridges are converted to slowly cycling latch bridges, the rate of detachment decreases, which is reflected by a decreasing V_{max} and η. Accordingly, in airway SM at the tissue level (activated by electric field stimulation), force, G′, and G″ rise sharply within the first 10 s, whereas both η and V_{max} transiently increase within 4 s but then decay in parallel with a time constant of ~20 s (7).

Although at the tissue level G′, G″, η, and their changes are thought to be governed primarily by actomyosin bridge dynamics, the actomyosin motors in cultured HASM cells must exert their effect in a cytoskeletal lattice, which is in a constant state of remodeling (8, 11, 17, 22, 26). Indeed, it is possible that the changes in cell mechanics that we observed might have been caused in part by nonbridge mechanisms. Changes in F-actin content, cell spreading, cytoskeletal tension, and cell adhesion have each been shown to affect stiffness in SM and other cell types (12, 21, 29). These mechanisms are not mutually exclusive, but we are unaware of any mechanism other than actomyosin bridge cycling that can explain both the fast and dramatic increase in cell stiffness and the η transient that is thought to be characteristic of bridge cycling rate regulation. Also, this argument does not preclude an important role for slower changes in cytoskeletal structure. For instance, the increase in η that we observed after treatment with DBcAMP (Fig. 4) has probably not been caused by an increase in bridge detachment rate. Instead, we hypothesize that DBcAMP causes a decrease in the number of actomyosin bridges, and, as their influence on η diminishes, η becomes dominated by frictional losses within the cytoskeleton. Conversely, an increase in the number of actomyosin bridges during contraction would increase their influence on η. Thus we favor the interpretation that the early changes in the mechanical properties of cultured HASM cells in response to contractile agonists reflect,

to an appreciable extent, the effect of actomyosin bridge dynamics.

Heterogeneity of responses. We found that HASM responded to histamine with changes in stiffness that ranged from no reaction in some cells up to a 33-fold increase in others (Fig. 5*A*). Similarly, cells responded to the bronchodilating agonist DBcAMP over a range from no relaxation to a 27-fold decrease in stiffness (Fig. 5*B*). This variability might be explained by a number of factors that can vary among cells, such as the amount of contractile proteins that is expressed (9, 10), density of receptors, concentration of free intracellular calcium, position of the bead on the cell, or the twisting direction of the bead relative to the principal axis of the cell body (4). It was beyond the scope of this report to elaborate on those factors. We found, however, a relationship between the magnitude of the mechanical responses and the baseline amplitude of bead displacement (Figs. 7 and 8). Softer cells stiffened more when challenged with histamine, and stiffer cells softened more in response to DBcAMP. A plausible explanation of these data is that stiffer cells tended to have a higher level of baseline tone and, as a consequence, could relax considerably but could not contract much more because they were already nearly maximally contracted. Conversely, softer cells tended to have a smaller baseline level of tone and thus could increase stiffness considerably when contracted but could not decrease stiffness much further when relaxed. This interpretation is supported by the following observation. The product of the increase in stiffness during contraction and the decrease during relaxation is the range over which cells can modulate their stiffness and characterizes the total contractile range of the cells. This range varied little (between 5.9- and 9.7-fold) in groups of cells that were ranked according to their baseline stiffness (Fig. 8). Thus total cell contractility (from maximally relaxed to maximally stimulated) was independent of baseline stiffness.

Variability of baseline tone among cells, however, was by itself insufficient to account for the wide variability of bead displacement amplitudes under baseline conditions (Fig. 4). Contractile or relaxing agonists that we expect to equalize the tone among cells (i.e., all cells become maximally contracted or maximally relaxed) only slightly reduced the geometric standard deviation of bead displacement amplitudes from 2.8 (baseline) to 2.5 (histamine) or to 2.6 (DBcAMP) (Fig. 4). Thus most of the heterogeneity of baseline bead displacement is not accounted for by differences in baseline tone between cells. Rather, we hypothesize that the wide distribution of bead displacement amplitudes is primarily attributable to heterogeneous attachment properties (e.g., contact area) between the bead and cell. A large contact area between the cell and bead, containing a large number of focal adhesion proteins and stress fibers, would be expected to decrease the bead displacement amplitude at a fixed torque. With the use of scanning electron microscopy, heterogeneous bead attachment properties have been demonstrated in cultured HASM cells, but also in bovine endothelial capillary cells, and are likely to occur in various other cell types (6). This might explain the wide distribution of bead displacements in response to lateral forces generated with magnetic tweezers that has been reported for mouse embryonic carcinoma cells (1) and fibroblasts (3). As a consequence of heterogeneous bead attachment properties, an absolute measure of the cell's elastic modulus cannot easily be obtained without a more detailed analysis of bead cell geometry and cell deformation. Nonetheless, the ratios G'/G'_0, G''/G'_0, and G''/G' (η) and ratios of bead displacement amplitudes (Figs. 2, 3, 5, 8) are normalized variables that reflect relative changes on a bead-by-bead basis and are, therefore, insensitive to details of bead attachment properties.

The heterogeneity of both the baseline stiffness and the mechanical response to agonists will have important consequences for future study design; to find significant differences in stiffness or contractility between two groups of cells, a large number of cells would need to be studied. For instance, an unpaired one-tailed *t*-test would require roughly 50 cells per group to detect differences of 25% in contractility or roughly 75 cells per group to detect differences of 25% in baseline stiffness. This requirement of large sample sizes could be problematic for techniques such as scanning probe microscopy or single-cell force measurements but imposes no difficulty for MTC with optical detection, as a single measurement contains data of typically 50 cells and experiments on over 1,000 cells can be completed within 1 day. The ability to measure the responses of individual beads could also be important for studies with transfected cells. Transfection efficiency in cell culture systems often remains below 20%, and averaging over transfected and nontransfected cells as done with conventional MTC would underestimate the effect to be investigated. If, however, cells are cotransfected with fluorescent proteins, their response could easily be distinguished from neighboring nontransfected cells using optical MTC.

In summary, we have measured the contractile response of individual SM cells in culture using a novel microrheology technique. We found that cultured SM cells express essential mechanical features that are characteristic of the contractile response at the tissue level, such as rapid increase in stiffness and transient increase in η after activation and decrease in stiffness after relaxation. In contrast to SM tissue, cultured cells have a more limited range over which they can regulate stiffness, and they exist in a partially contracted state (tone) under baseline conditions. This baseline tone, however, varied among cells, which contributed appreciably to a wide distribution of responses to contractile or relaxing agonists.

We thank Winfried Möller and Maureen Harp for help with bead production, Claude Duvivier and Luc Eberhard for technical assistance, and Rick Rogers for support with microscopy.

This work was supported by National Heart, Lung, and Blood Institute Grant PO1 HL-33009.

REFERENCES

1. **Alenghat FJ, Fabry B, Tsai KY, Goldmann WH, and Ingber DE.** Analysis of cell mechanics in single vinculin-deficient cells using a magnetic tweezer. *Biochem Biophys Res Commun* 277: 93–99, 2000.
2. **Barany M.** ATPase activity of myosin correlated with speed of muscle shortening. *J Gen Physiol* 50, *Suppl*: 197–218, 1967.
3. **Bausch AR, Ziemann F, Boulbitch AA, Jacobson K, and Sackmann E.** Local measurements of viscoelastic parameters of adherent cell surfaces by magnetic bead microrheometry. *Biophys J* 75: 2038–2049, 1998.
4. **Butler JP and Kelly SM.** A model for cytoplasmic rheology consistent with magnetic twisting cytometry. *Biorheology* 35: 193–209, 1998.
5. **Draeger A, Stelzer EH, Herzog M, and Small JV.** Unique geometry of actin-membrane anchorage sites in avian gizzard smooth muscle cells. *J Cell Sci* 94: 703–711, 1989.
6. **Fabry B, Maksym GN, Hubmayr RD, Butler JP, and Fredberg JJ.** Implications of heterogeneous bead behavior on cell mechanical properties measured with magnetic twisting cytometry. *J Magnetism Magnetic Materials* 194: 120–125, 1999.
7. **Fredberg JJ, Jones KA, Nathan M, Raboudi S, Prakash YS, Shore SA, Butler JP, and Sieck GC.** Friction in airway smooth muscle: mechanism, latch, and implications in asthma. *J Appl Physiol* 81: 2703–2712, 1996.
8. **Gunst SJ, Meiss RA, Wu MF, and Rowe M.** Mechanisms for the mechanical plasticity of tracheal smooth muscle. *Am J Physiol Cell Physiol* 268: C1267–C1276, 1995.
9. **Halayko AJ, Salari H, Ma X, and Stephens NL.** Markers of airway smooth muscle cell phenotype. *Am J Physiol Lung Cell Mol Physiol* 270: L1040–L1051, 1996.
10. **Halayko AJ and Solway J.** Molecular mechanisms of phenotypic plasticity in smooth muscle cells. *J Appl Physiol* 90: 358–368, 2001.
11. **Hirshman CA and Emala CW.** Actin reorganization in airway smooth muscle cells involves G_q and G_{i-2} activation of Rho. *Am J Physiol Lung Cell Mol Physiol* 277: L653–L661, 1999.
12. **Hubmayr RD, Shore SA, Fredberg JJ, Planus E, Panettieri RA Jr, Möller W, Heyder J, and Wang N.** Pharmacological activation changes stiffness of cultured human airway smooth muscle cells. *Am J Physiol Cell Physiol* 271: C1660–C1668, 1996.
13. **Huxley AF.** Muscle structure and theories of contraction. *Prog Biophys Biophys Chem* 7: 255–318, 1957.
14. **Ishida K, Pare PD, Hards J, and Schellenberg RR.** Mechanical properties of human bronchial smooth muscle in vitro. *J Appl Physiol* 73: 1481–1485, 1992.
15. **Laporte JD, Moore PE, Panettieri RA, Moeller W, Heyder J, and Shore SA.** Prostanoids mediate IL-1β-induced β-adrenergic hyporesponsiveness in human airway smooth muscle cells. *Am J Physiol Lung Cell Mol Physiol* 275: L491–L501, 1998.
16. **Maksym GN, Fabry B, Butler JP, Navajas D, Tschumperlin DJ, Laporte JD, and Fredberg JJ.** Mechanical properties of cultured human airway smooth muscle cells from 0.05 to 04 Hz. *J Appl Physiol* 89: 1619–1632, 2000.
17. **Mehta D and Gunst SJ.** Actin polymerization stimulated by contractile activation regulates force development in canine tracheal smooth muscle. *J Physiol (Lond)* 519: 829–840, 1999.
18. **Möller W, Stahlhofen W, and Roth C.** Improved spinning top aerosol generator for the production of high concentrated ferrimagnetic aerosols. *J Aerosol Sci* 21: S435–S438, 1990.
19. **Moore PE, Laporte JD, Gonzalez S, Möller W, Heyder J, Panettieri RA Jr, and Shore SA.** Glucocorticoids ablate IL-1β-induced β-adrenergic hyporesponsiveness in human airway smooth muscle cells. *Am J Physiol Lung Cell Mol Physiol* 277: L932–L942, 1999.
20. **Panettieri RA, Murray RK, DePalo LR, Yadvish PA, and Kotlikoff MI.** A human airway smooth muscle cell line that retains physiological responsiveness. *Am J Physiol Cell Physiol* 256: C329–C335, 1989.
21. **Pourati J, Maniotis A, Spiegel D, Schaffer JL, Butler JP, Fredberg JJ, Ingber DE, Stamenovic D, and Wang N.** Is cytoskeletal tension a major determinant of cell deformability in adherent endothelial cells? *Am J Physiol Cell Physiol* 274: C1283–C1289, 1998.
22. **Pratusevich VR, Seow CY, and Ford LE.** Plasticity in canine airway smooth muscle. *J Gen Physiol* 105: 73–94, 1995.
23. **Rayment I, Holden HM, Whittaker M, Yohn CB, Lorenz M, Holmes KC, and Milligan RA.** Structure of the actin-myosin complex and its implications for muscle contraction. *Science* 261: 58–65, 1993.
24. **Shore SA, Laporte J, Hall IP, Hardy E, and Panettieri RA Jr.** Effect of IL-1β on responses of cultured human airway smooth muscle cells to bronchodilator agonists. *Am J Respir Cell Mol Biol* 16: 702–712, 1997.
25. **Shue GH and Brozovich FV.** The frequency response of smooth muscle stiffness during Ca2+-activated contraction. *Biophys J* 76: 2361–2369, 1999.
26. **Togashi H, Emala CW, Hall IP, and Hirshman CA.** Carbachol-induced actin reorganization involves G_i activation of Rho in human airway smooth muscle cells. *Am J Physiol Lung Cell Mol Physiol* 274: L803–L809, 1998.
27. **Valberg PA and Butler JP.** Magnetic particle motions within living cells. Physical theory and techniques. *Biophys J* 52: 537–550, 1987.
28. **Wang N, Butler JP, and Ingber DE.** Mechanotransduction across the cell surface and through the cytoskeleton. *Science* 260: 1124–1127, 1993.
29. **Wang N and Ingber DE.** Control of cytoskeletal mechanics by extracellular matrix, cell shape, and mechanical tension. *Biophys J* 66: 2181–2189, 1994.
30. **Warshaw DM and Fay FS.** Tension transients in single isolated smooth muscle cells. *Science* 219: 1438–1441, 1983.
31. **Warshaw DM, Rees DD, and Fay FS.** Characterization of cross-bridge elasticity and kinetics of cross-bridge cycling during force development in single smooth muscle cells. *J Gen Physiol* 91: 761–779, 1988.